Tellus (2004), 56B, 93–104
Printed in UK. All rights reserved

TELLUS

Optimal determination of the parameters controlling biospheric CO_2 fluxes over Europe using eddy covariance fluxes and satellite NDVI measurements

By TUULA AALTO[1]*, PHILIPPE CIAIS[2], ANNE CHEVILLARD[3] and CYRIL MOULIN[2],
[1]*Finnish Meteorological Institute, Air Quality Research, Sahaajankatu 20E, 00880 Helsinki, Finland;* [2]*Laboratoire des Sciences du Climat et de l'Environnement, UMR CEA-CNRS 1572, F-91198 Gif-sur-Yvette cedex, France;*
[3]*DPRE/SERGD/LEIRPA, CEA Fontenay-aux-Roses, 18, Rue du Panorama (BP6), 92265 Fontenay-aux-Roses, France*

(Manuscript received 17 July 2002; in final form 20 October 2003)

ABSTRACT

Ecosystem CO_2 flux measurements using the eddy covariance method were compared with the biospheric CO_2 exchange estimates of a regional scale atmospheric model. The model described the seasonal patterns quite well, but underestimated the amplitude of the fluxes, especially at the northern sites. Two model parameters, photosynthetic efficiency for light use and Q_{10} for soil respiration, were re-evaluated on a diurnal and seasonal basis using the results from flux measurements. In most cases the photosynthetic efficiency was higher than the earlier estimate. The resulting flux was very sensitive to the value of photosynthetic efficiency, while changes in Q_{10} did not have a significant effect.

1. Introduction

Studies of atmospheric carbon dioxide are an important part of current climate change research. Models of different scales have been constructed in order to simulate the fluxes of carbon over land and ocean surfaces, and their variability (e.g. McGuire et al., 2001; Pacala et al., 2001; Gurney et al., 2002). Those models can be connected to and validated or calibrated against direct carbon flux measurements. Satellite observations have also been used to quantify the CO_2 exchange by the vegetation at global and regional scales, since they deliver homogenous, repetitive and global coverage measurements of the surface reflectances, which can be inverted into products such as normalized difference vegetation index (NDVI), leaf area index (LAI) and fraction of absorbed photosynthetically active radiation (FAPAR) that are directly related to canopy photosynthesis (e.g. Maisongrande et al., 1995; Kindermann et al., 1996). On a smaller scale, ecosystem level fluxes can now be measured accurately by the eddy covariance technique (Valentini et al., 2000; Baldocchi et al., 2001). Those different approaches, namely eddy covariance measurements, satellite data and biomass inventories, can be combined to estimate the terrestrial sink or sources of carbon (e.g. Cramer et al., 1999).

In this study we compare the results of a "light-use efficiency" model of net ecosystem exchange (NEE) driven by satellite and climate observation with pointwise NEE measurements by eddy covariance. The model is corrected to best match the measurements, when necessary, via an optimization of its parameters. Ecosystem-level NEE measurements are a powerful tool for evaluating model behaviour (Ruimy et al., 1996b; Cramer et al., 1999), yet they are relatively little exploited considering the amount of existing material. The measurements of NEE utilized in this work have been made at 13 flux tower sites in Europe operated under the EUROFLUX project and by the Finnish Meteorological Institute (Valentini et al., 2000; Aurela et al., 2001a,b). The model, called TURC (for Terrestrial Uptake and Release of Carbon), utilizes satellite NDVI and climate *in situ* time-series co-located with eddy covariance flux measurements in order to estimate NEE, based on a light-use efficiency formulation (Ruimy et al., 1996a; Lafont et al., 2002). The TURC model was applied originally to calculate the global distribution of NEE, which has been transported into regional and global scale atmospheric models (Chevillard et al., 2002; Ciais et al., 2002) and compared with continuous records of atmospheric CO_2. Here we are only concerned about the performance of TURC at the local scale, although for several sites that are representative of a large variety of European forest ecosystems.

*Corresponding author.
e-mail: tuula.aalto@fmi.fi

In the current study, the modelled and measured NEE are compared over one growing season on an hourly basis. We interpret the mismatch between the simulation and the observation to result from the setting of four key model parameters in TURC: the light-use efficiency (ε), the dependence of soil respiration on soil temperature (Q_{10}), the specific soil respiration rate (V_0) and the intensity of plant maintenance respiration. Optimized values for ε and Q_{10} are obtained by minimizing the distance between model output and observation. The quality of the parameter retrieval and the resulting optimized estimates are studied on a daily and seasonal basis.

2. Materials and methods

2.1. Eddy covariance NEE measurements

By convention NEE is taken in the following as negative when CO_2 leaves the atmosphere. The NEE measurements come from the EUROFLUX database (see http://www.fluxnet.ornl.gov/fluxnet/eurointro.cfm) and the Finnish Meteorological Institute (Aurela et al., 2001a,b). Measurements at 13 sites over Europe were utilized, ranging from southern France to northern Finland (Table 1). The measured forests consisted of coniferous, broad-leaved deciduous and mixed species. They span over an annual temperature range of 15 °C between 44 and 69 degrees of latitude. Both natural and planted stands were included. The measurements were made using automated eddy covariance technique (e.g. Aubinet et al., 2000). The selected time period covered the growing season of 1998, except for FI4 (1996). The measured eddy flux on top of the canopy was used instead of the true NEE, that is storage terms below the eddy covariance system which can become important during night-time were ignored. Nevertheless, we use only "elite" flux data during well-mixed conditions ($u^* > 0.2$ m s^{-1}).

2.2. Satellite NDVI measurements

We used NDVI data from SPOT4-VEGETATION spaceborne instrument to monitor the vegetation cycle over the course of the year at the different stations. Ten-day syntheses (the so-called "S10 VEGETATION product") are available on internet from the Flemish Institute for Technological Research (VITO) Image Processing and Archiving Centre (http://www.vgt.vito.be/indexstart.htm). These maps are projected on a regular latitude–longitude grid with a 1 km resolution. The NDVI global time series is a 10-day composite value obtained by sampling the highest NDVI within 10 consecutive days and among four neighbouring pixels in the original 1 km VEGETATION dataset. Thus, the timing of photosynthesis as driven by NDVI cannot be more precisely determined than a 10-day error. A 10-day NDVI map is made of the "best" measurements performed during the period. The "best" measurement is basically the non-cloudy pixel with the highest NDVI value to avoid snow contamination. The VEGETATION NDVI is computed from top-of-atmosphere radiance after atmospheric correction. Because cloudy or snowy conditions may well persist over a 10-day period, and because no spatial or temporal interpolation is performed on these products, the syntheses contain some cloudy or snowy pixels that have to be removed. We achieved this by using information provided by the Status Map, a companion file that comes with the NDVI 10-day synthesis file.

2.3. Light-use efficiency NEE model

We used the TURC model initially developed by Ruimy et al. (1996a), and later modified by Lafont et al. (2002). In TURC, the NEE is estimated using climate and NDVI. The main modifications made by Lafont et al. (2002) consist of a new calibration of the model via the light-use efficiency parameter (see below),

Table 1. Site characteristics. Species: 1, Betula nana; 2, Betula pubescens; 3, Fagus sylvatica; 4, Larix decidua; 5, Picea abies; 6, Picea sitchensis; 7, Pinus pinaster; 8, Pinus sylvestris; 9, Pseudotsuga menziesii; 10, Quercus robur

Site	Location	Species	LAI	Age	$T_{\text{annualmean}}$	Reference
France1 (FR1)	44°05′N 0°05′E	7	5.5	25	13.5	Berbigier et al. (2001)
France2 (FR2)	48°40′N 7°05′E	3	6	30	9.2	Granier et al. (2000)
Germany1 (GE1)	50°09′N 11°52′E	5	5	48	5.8	Valentini (2003)
Belgium1 (BE1)	50°18′N 6°00′E	5, 3, 9	4.5	60–90	7	Valentini (2003)
Germany2 (GE2)	50°58′N 13°38′E	5, 4	6	99	7.5	Valentini (2003)
Belgium2 (BE2)	51°18′N 04°31′E	8, 10	3	70	10	Kowalski et al. (1999)
United Kingdom1 (UK1)	56°37′N 3°48′W	6	8	14	8	Valentini (2003)
Sweden1 (SW1)	60°05′N 17°28′E	5, 8	5	80–100	5.5	Lindroth et al. (1998)
Finland1 (FI1)	61°51′N 24°17′E	8	3	35	3.5	Markkanen et al. (2001)
Sweden2 (SW2)	64°14′N 19°46′E	5	2	31	1	Valentini (2003)
Finland2 (FI2)	67°58′N 24°07′E	5, 8, 2	2	>30	−1.6	Aalto et al. (2002)
Finland3 (FI3)	69°08′N 27°17′E	wetland	0.7		−2.0	Aurela et al. (2001a)
Finland4 (FI4)	69°28′N 27°14′E	1	2.5	>40	−2.0	Aurela et al. (2001b)

and in the use of NDVI data from the SPOT4-VEGETATION space-borne instrument instead of NOAA-AVHRR in the original version. In the TURC model, NEE is given by

$$\mathrm{NEE} = -W + Rm + Rg + Rs \tag{1}$$

where W is canopy photosynthesis and Rm, Rg and Rs are respectively plant maintenance, growth and soil respiration. The hourly gross canopy photosynthesis (W in μmol CO_2 m^{-2} s^{-1}) is given by

$$W = f\varepsilon gcI \tag{2}$$

where I the incident solar global radiation (W m^{-2}), c is a more or less constant factor used to convert from global radiation to quanta in the photosynthetically active region (PAR) of the spectrum (2.2 molPAR MJ^{-1}), g is a freezing factor (dimensionless), ε is the light-use efficiency of the canopy (molCO_2 molPAR^{-1}), and f is the absorption coefficient of PAR in the canopy (dimensionless). All quantities in eq. (1) are calculated as daily means, except for I which is used on an hourly basis. The photosynthetic efficiency ε was set by Lafont et al. (2002) from linear regression between instant flux measurements (two data points belong to the EUROFLUX dataset and others are independent) and annual mean temperature. The absorption coefficient f depends linearly on the NDVI which is computed from satellite observations (Ruimy et al., 1994; Maisongrande et al., 1995). However, NDVI may saturate when observing dense vegetation, and accordingly f will be underestimated (Eklundh et al., 2001). In order to take this into account, f is adjusted according to local LAI determined during growing season peak (from EUROFLUX database). The maximum value of f during the growing season is calculated from $f = 0.95 \times [1 - \exp(-0.6 \times \mathrm{LAI})]$ (Lafont et al., 2002) and the rest of the values are scaled linearly (NDVI changed by less than 30% over the high growing season). The freezing factor g is applied to divide W by two when the daily average of air temperature is lower than -2 °C for more than three consecutive days.

The release of CO_2 by respiratory processes is divided into autotrophic (plant) respiration and heterotrophic (soil) respiration. Autotrophic respiration is further separated into maintenance respiration (Rm) and growth respiration (Rg) that are expressed as follows:

$$\begin{aligned} Rm &= aT + b \\ Rg &= 0.28(W - Rm), \end{aligned} \tag{3}$$

where T is the air temperature and a and b are functions of plant biomass (leaves, wood and roots) being expressed on a daily basis. Rg is updated daily, and $Rg = 0$ if W–Rm is negative because growth respiration appears only if there are enough photosynthesis products for further processing. Soil respiration (Rs) is defined as the CO_2 production resulting from the respiration of soil organisms and mycorrhizae and it is expressed through a Q_{10} relationship (Raich and Schlesinger, 1992):

$$Rs = V_0 Q_{10}^{\frac{(T_{\mathrm{soil}} - T_0)}{10}}, \tag{4}$$

where T_0 is a reference temperature set to 0 °C, T_{soil} is the soil temperature; Q_{10} the dependence of soil respiration on soil temperature, is set to 2.0, and does not vary in time or space. The product V_0 of soil carbon density (molC m^{-2}) by a specific respiration rate (s^{-1}) is treated as a single model parameter which can be adjusted for example to set NEE = 0 on an annual basis or to adapt to specific environmental conditions (e.g. drought).

Radiation and temperature input data used to force the TURC model were taken from the EUROFLUX site measurements rather than from a numerical weather prediction model, as in former global applications of the model, because using the observed meteorology enables more accurate comparison with the pointwise flux tower measurements and reparametrization of TURC. The flux modelling period extended from April 1998 to October 1998.

3. Inversion procedure

The TURC model parameters were optimized by minimizing the distance between modelled and measured fluxes, weighted by the data and the parameter errors. Both diurnal and seasonal inversion of the TURC parameters were attempted. NEE is the sum of photosynthesis, which can be adjusted via the photosynthetic efficiency ε, and respiration which can be optimized by changing the parameters a, b, V_0 and Q_{10}. Q_{10} was our main goal here, but it turned out to be unrealistic to try to attribute all the differences between model and observations to Q_{10} alone. Thus, the respiration terms were changed by also re-estimating V_0 for soil respiration and adding a single parameter C, a multiplier for a and b which simply allows linear adjustment of maintenance respiration. The re-estimation procedure thereby included four parameters (ε, V_0, Q_{10} and C).

3.1. *Cost function*

The minimization procedure can be performed by calculating a cost function J for each site (e.g. Tarantola, 1994; Barlow, 1993). The first term in J represents the distance between modelled and measured quantities, weighted by the measurement error:

$$J = \frac{1}{2} \sum_{j=1}^{P} \sum_{i=1}^{N} \frac{[G_i(p_j) - O_i]^2}{\sigma_{\mathrm{obs},i}^2} + \frac{1}{2} \sum_{j=1}^{P} \frac{(p_j - \hat{p}_j)^2}{\sigma_{P,j}^2}, \tag{5}$$

where for the time step i, $G_i(p_j)$ is the modelled NEE as a function of $P = 4$ parameters, O_i the observed NEE and $\sigma_{\mathrm{obs},i}$ the variation of the flux. Summation is made over weekly composite hours during the growing season. The variation of the flux σ_{obs} is a vector calculated as the standard deviation of the seven hourly fluxes entering in each weekly composite datum. σ_{obs} was

usually about 10% of the measured flux. The estimated parameters were not very sensitive to σ_{obs}. An increase in σ_{obs} by a factor of 2 during the night did not cause any effect, while the same increase applied to daytime data changed the solution by <10%. Solving for annual mean parameters implies that $P = 4$ unknown parameters are constrained by $N = 52 \times 24 = 1248$ data points. Solving for daily parameters implies that, for every day, $P = 4$ parameters are constrained by 24 data points. The second term in J is a Bayesian term which contains the distance between the optimized parameters and its *a priori* value $\hat{p}$. An *a priori* error σ_p is assigned to each parameter in the Bayesian formalism. A large value for σ_p means that a loosely constrained parameter acts to lower the cost function J.

3.2. Error estimates on parameters

An error was calculated for the parameter estimates using Monte Carlo inverse simulations (see e.g. Tarantola, 1994). The measurement errors were normally distributed. A new time-series of fluxes was created by adding a random component to the original fluxes. The random component was created by multiplying a zero-centred normally distributed random number by standard deviation of the fluxes. This was repeated 10 000 times and thus a large simulated set of NEE pseudo data was obtained with same standard deviation and mean as the original one. A set of optimized parameters was solved for each flux time-series.

4. Results

4.1. Results of the direct model

The measured and modelled NEE are presented in Fig. 1 as weekly composites at two selected sites in Eastern France (Fagus Sylvatica) and Southern Finland (Pinus Sylvestris). High NEE is observed to occur roughly from the beginning of May to the end of August. At high northern latitudes, the period of maximum carbon uptake is very short and spans roughly from the beginning of July to mid August. Despite the fact that the TURC model captures well the timing of maximum NEE (model minus observed timing <4 weeks)- in summer, the spring-time onset is modelled to occur several weeks later than observed at FR1, UK1, BE1 and BE2 and earlier than observed at FR2 and FI3. Besides deficient representation of the phase of the seasonal cycle, the model underestimates the NEE amplitude at several sites (Fig. 2). We used the maximum NEE during the growing season (NEE_{max}) as an indicator of the ability of TURC to simulate the NEE seasonal amplitude. Maximum NEE was computed at each site by first finding the single largest hourly flux for each day during the growing season and then averaging the 10 highest fluxes found. Figure 2 demonstrates that TURC overestimates NEE_{max} by less than 30% at southern sites (FR1, GE1) and underestimates it by up to 67% at northern sites (e.g. SW1, FI1, SW2, FI2, FI3). The most probable candidate parameter in TURC for re-evaluation is the photosynthetic efficiency ε. It can

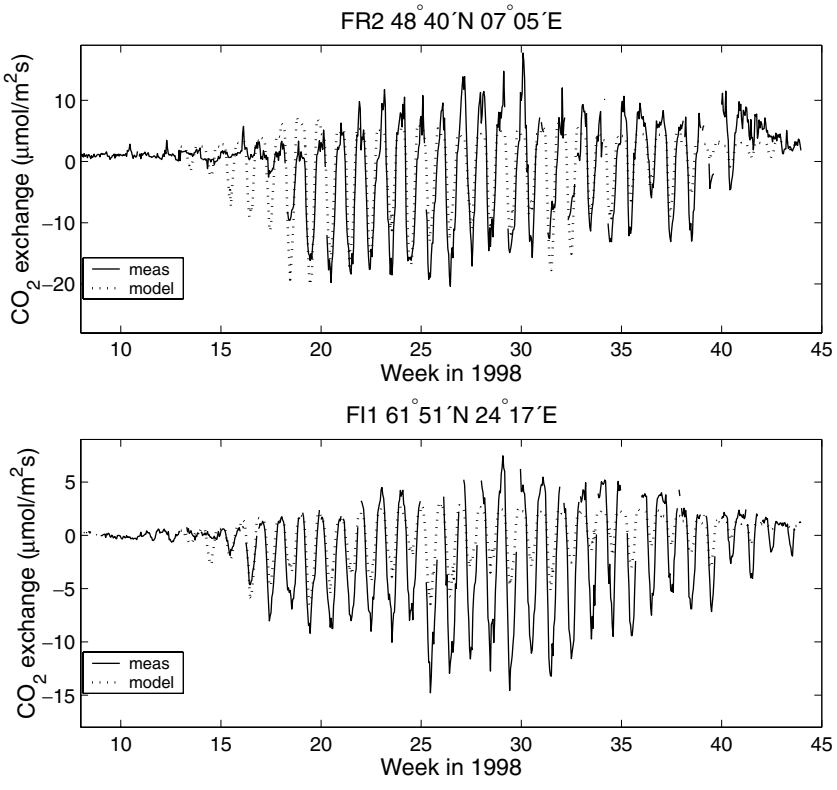

Fig. 1. Weekly composite fluxes according to model and measurements during growing season 1998. Weekly composites refer to mean of hourly fluxes during one week, i.e. 7-point mean for each hour over the daily cycle.

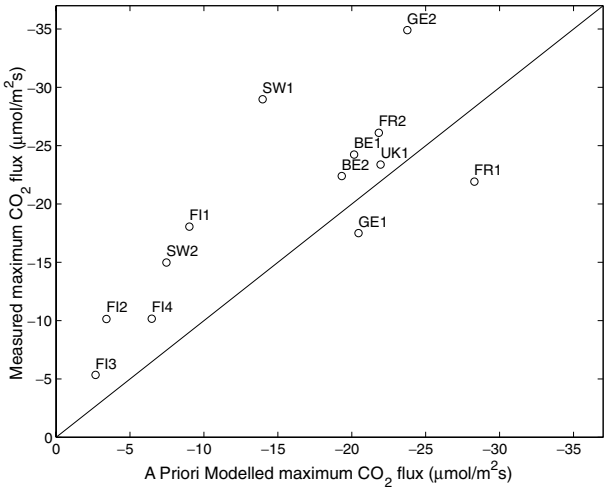

Fig. 2. Maximum CO_2 uptake rate according to model and measurements. Site codes are listed in Table 1.

also be seen in Fig. 1 that NEE_{max} is too small at FI1 because the values at noon are too small, that is the diurnal cycle amplitude is underestimated for several consecutive weeks, which impacts upon the seasonal amplitude. The value of ε may vary according to tree species, nutrition, water stress (Prince, 1991; Jarvis and Leverenz, 1983) and diffuse to direct fraction in solar irradiance (Roderick et al., 2001), in addition to annual mean temperature alone as hypothesized by Lafont et al. (2002). The temperature dependency Q_{10} of soil respiration may also need adjustment. It was assumed constant by Lafont et al. (2002) but may actually be higher in colder climates (Lloyd and Taylor, 1994; Valentini et al., 2000), or increase during the growing season together with a larger contribution from root respiration (Boone et al., 1998).

4.2. *Results of the inverse model*

4.2.1. Light-use efficiencies. In a first set of inversions, daily values of ε were solved by minimizing eq. (5), and their errors were calculated by the Monte Carlo method detailed above. The daily values of ε are shown as an example for UK1 in Fig. 3. In April, at the onset of the growing season, there is a large mismatch between the *a priori* model and the data, which forces higher ε values in the optimization procedure. A clear spring bias of TURC in the same direction is also found at sites FR1 and BE2. A bias in the opposite direction is found at FR2, FI1, SW2, FI3 and FI4, resulting in significantly lower optimized ε. Small biases also occurred during the autumn at a few sites. At UK1, the air temperature increased to near 10 °C by the beginning of April and dropped again to near 0 °C by mid April (see insert in Fig. 3). Before and right after the cold event in mid April, the temperature was high enough to sustain photosynthesis which could be seen in the eddy covariance measurements, but not as well on the 10 d composited NDVI values. At FI1 and SW2 the soil was frozen until the beginning of May. The NDVI were already significantly elevated before that time, but the measured fluxes followed NDVI at full intensity only after thawing of the soil.

In a second set of inversions, a "seasonal average" value of light-use efficiency, referred here to as $\bar{\varepsilon}$, was solved over the period of highest carbon uptake. This so-called "high growing season" generally spans from May to August, but at northernmost sites it only lasts from the beginning of July to mid August. The length of the period chosen for inverting $\bar{\varepsilon}$ was also affected by gaps in the time-series (Table 2). The optimized $\bar{\varepsilon}$ values are given in Table 2 and shown in Fig. 4 as a function of the mean annual temperature and latitude. We note that the optimized $\bar{\varepsilon}$ is changed by a factor of 0.8–2.8 from those assigned by Lafont et al. (2002). The largest change in $\bar{\varepsilon}$ is obtained for FI3. This results from the very low local LAI used in the analysis (0.7 on average for the vascular plants in the peatland hollows and hummocks), which leads to low modelled fluxes. We note that the fit to the data, especially in spring, is not as good with seasonal mean $\bar{\varepsilon}$ as with daily ε.

4.2.2. Temperature dependence of the soil respiration Q_{10}. A seasonal average value for $\bar{Q}_{10}$ at each site was optimized against the weekly composite NEE data during the high growing season. Errors were deduced from the Monte Carlo simulations as explained above. The results are shown in Fig. 4 and Table 2. The *a posteriori* error in $\bar{Q}_{10}$ is large, of the order of 100% of the mean, and the error reduction from the prior did not exceed a few % (against 70% in the case of parameter ε). This indicates that the $\bar{Q}_{10}$ parameter is not well constrained by NEE observations. At the same sites where the optimization resulted in an increase in photosynthetic efficiency (e.g. SW1, UK1) we also found that optimized $\bar{Q}_{10}$ values were higher than the *a priori* ones. The optimized $\bar{Q}_{10}$ does not show a significant increase towards low annual temperatures across the transect of EUROFLUX stations, and inverting $\bar{Q}_{10}$ independently or not from V_0 does not change the result. Janssens et al. (2001) fitted $\bar{Q}_{10}$ from night-time fluxes and soil temperatures. The $\bar{Q}_{10}$ obtained using this "classic" method are shown for comparison in Fig. 4. They compare within their errors with our estimates and suggest that $\bar{Q}_{10}$ might increase with colder temperatures. We attempted to optimize daily values of Q_{10}, but in that set of inversions we found that hourly NEE observations helped little in constraining a daily Q_{10} which sets the dependency of soil respiration on soil temperature, a variable that has practically no diurnal cycle (Fig. 5). Therefore, optimized daily Q_{10} were plagued by very large uncertainties, not to speak of day to day variability and gaps in the eddy covariance data. At FI3, the daily optimized Q_{10} show an increase from the *a priori* value of 2 to values of about 3.5 in the spring and autumn. The reason for this is that the *a priori* modelled uptake is higher than observed so that soil respiration gets increased in the inversion to reduce that mismatch. At southern sites the model indicated low respiration rates due to the poor ability of the model to adjust to night-time

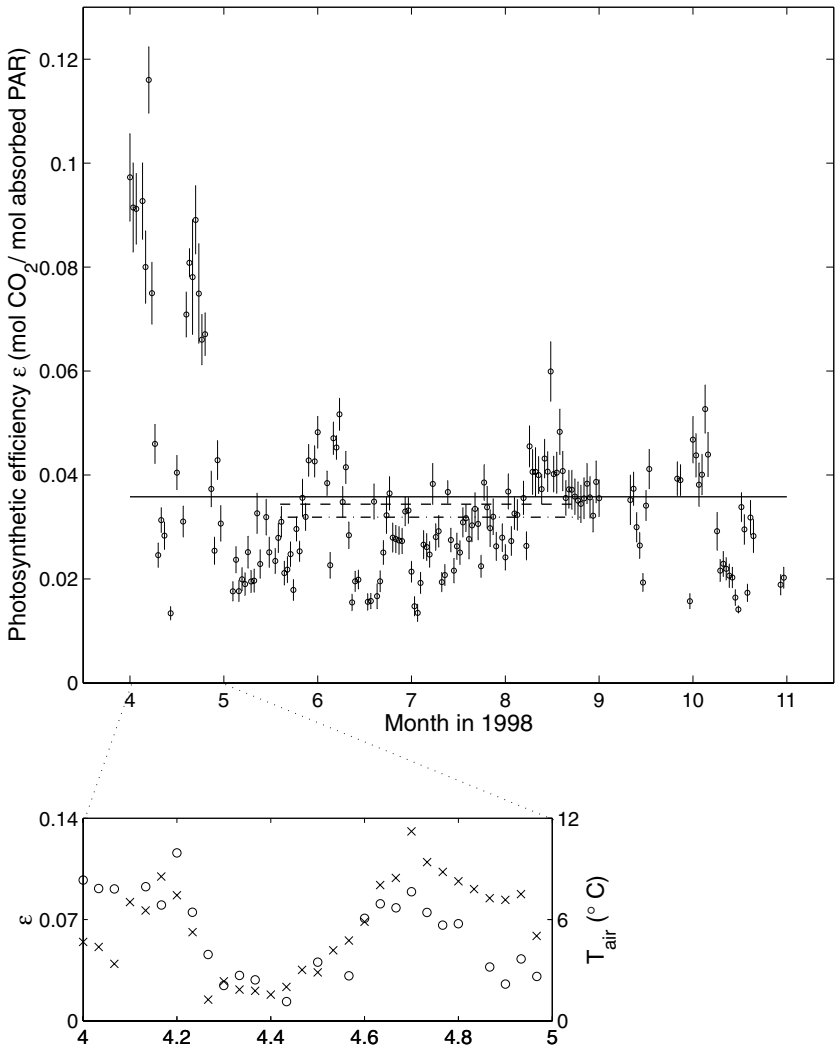

Fig. 3. Daily optimized values of ε at the site UK1 (see Table 1 for site details). The solid line refers to the average of daily ε and the dashed line to the high growing season constant ε. The dashed-dotted line refers to the average of daily ε during the high growing season. Crosses in the inset refer to daily average temperatures.

Table 2. Optimized parameters ε and Q_{10} and corresponding error estimates for NEE from April to October. *hgs* refers to high growing season values and *dm* to mean of daily values. χ^2_{orig} refers to the error estimate using the original set of parameters

	χ^2_{orig}	ε_{hgs}	$Q_{10\,\text{hgs}}$	χ^2_{hgs}	hgs period (weeks)	ε_{dm}	$Q_{10\,\text{dm}}$	χ^2_{dm}
FR1	2.51	0.0160	1.92	1.30	20–25	0.0285	1.46	0.77
FR2	4.77	0.0159	1.81	4.70	20–34	0.0185	1.85	1.61
GE1	1.05	0.0147	2.15	0.93	20–31	0.0173	2.03	0.76
BE1	1.41	0.0186	1.88	1.06	20–34	0.0286	1.42	0.62
GE2	1.33	0.0291	1.93	0.62	20–34	0.0364	1.75	0.50
BE2	1.03	0.0217	2.08	0.93	24–34	0.0253	2.01	0.55
UK1	1.87	0.0266	2.60	1.01	20–34	0.0345	2.33	0.61
SW1	1.71	0.0343	2.80	0.54	26–34	0.0386	3.39	0.49
FI1	1.93	0.0277	2.30	1.40	20–34	0.0350	2.39	0.97
SW2	1.98	0.0255	2.40	1.33	21–34	0.0335	2.44	0.88
FI2	3.13	0.0235	1.95	1.19	28–29	0.0221	1.01	1.17
FI3	10.67	0.0262	1.57	3.33	26–33	0.0245	2.13	3.27
FI4	2.28	0.0156	2.26	0.89	27–33	0.0164	2.81	0.50

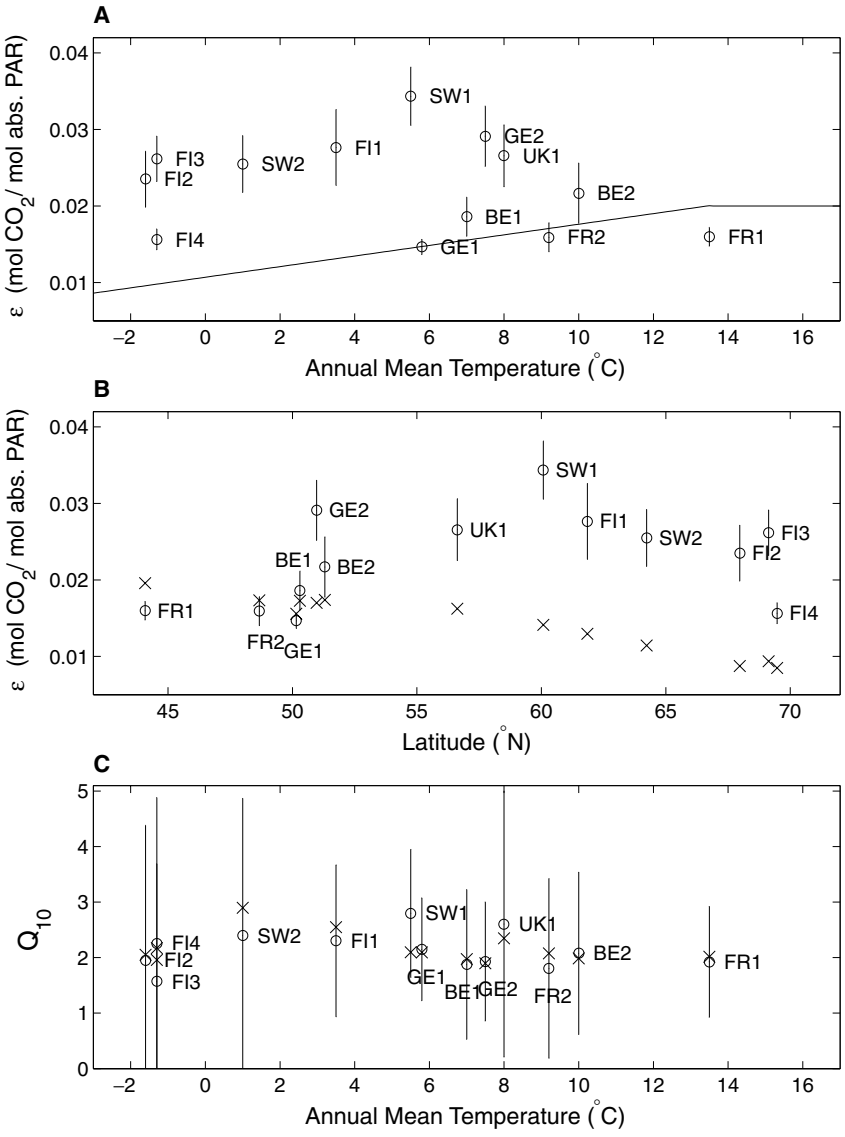

Fig. 4. A: Optimized photosynthetic efficiencies for the individual sites using high growing season measurements (circles). The error bar corresponds to the *a posteriori* error returned by the inverse procedure. The solid line refers to the temperature-dependent function that was *a priori* chosen to determine ε as a function of mean annual temperature in the model. B: The optimized photosynthetic efficiency versus latitude. Crosses refer to original values for ε. C: Optimized Q_{10} using high growing season NEE observations for individual sites. Crosses refer to Q_{10} values fitted to measurements of soil temperature and night-time fluxes (complete data sets used).

NEE values. The NEE measurements often indicate low respiration rates in the evening and high rates in the morning, while the model driven by soil temperature predicts a relatively uniform respiration rate throughout the night. This mismatch may partly reflect a missing storage correction in the measurements.

4.2.3. Quality of the inversion. The quality of the inversion procedure was evaluated using the optimized value of the cost function J. Bayesian optimization theory points to the fact that $\chi^2 = 2J/N$ follows χ^2 statistics, where N is the number of measurements or independent degrees of freedom, and that the estimated parameters are reliable only if χ^2 takes values close to 1. A value of χ^2 higher than 1 reflects that the solution is too much influenced by the prior, due, for instance, to "optimistic" tight prior errors on parameters. Values of χ^2 lower than 1 are conversely too "pessimistic", but at least in that case the parameter estimate is predominantly inferred from the observations rather than from the prior, which is preferable. The criterion of χ^2 close to 1 was verified in all the results discussed here.

Because of the Bayesian term, the inversion depends on priors, and it is important to check that the solution is not nudged to the priors because of tight prior error σ_p. Optimized values of the parameters were solved for several values of the *a priori* error σ_p. There is in theory no way to assign a value to the prior error, except from knowledge of the geophysical system that is modelled. Nevertheless, one can examine how J depends on σ_p (see e.g. Tarantola, 1994). The inverted parameters usually became unrealistic when σ_p increased, whereas J and $\partial J/\partial\sigma_p$ usually decreased while σ_p increased. The value of $\partial J/\partial\sigma_p$ should be small enough so that further changes in σ_p do not change the modelled flux considerably (the accuracy is determined by the measurement error). Thus, a value was assigned for σ_p such as J and $\partial J/\partial\sigma_p$ were as low as possible and parameters were

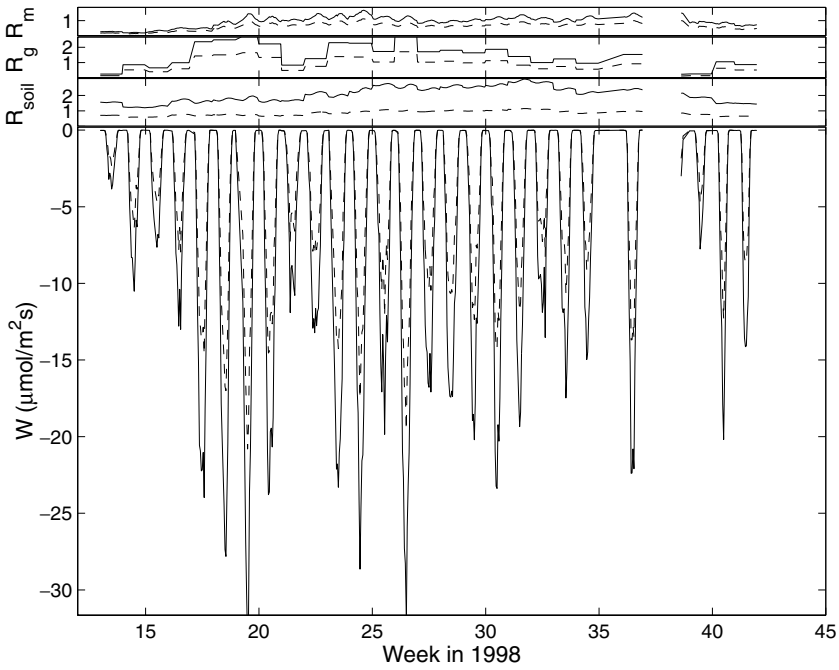

Fig. 5. Modelled CO_2 assimilation rate and respiration (eqs. (1)–(4)) as weekly composites for UK1. Solid curves refer to the optimized rates and dashed curves to *a priori* rates.

realistic. The rate of change of J, $\partial J/\partial\sigma_p$, was usually less than 2% at values higher than 5 for σ_p. On average, a change of this magnitude modifies the modelled flux by less than σ_{obs}, the measurement error, which indicates that further increase in σ_p could not significantly improve the fit. A value of 5 for σ_p was used as a standard for inverting daily values in parameters. In order to verify the validity of the minimization procedure, at site UK1 we performed an ensemble of inversions where different values for $\hat{p}$ were tested in such a manner that the innovation vector $G(\hat{p}) - O$ is null on average. The same solution for the inverted parameter set was found regardless of the value of $\hat{p}$ within a range that is considerably larger than the range found for the optimized parameters.

A distribution of optimized parameter values was obtained from the Monte Carlo simulations (Fig. 6). They were usually normally distributed, so that the *a posteriori* error on a parameter was taken as the standard deviation of the distribution. The distribution of optimized Q_{10}, however, was sometimes of logarithmic type and the value where the number of incidents decreased to 1/e of the largest number of incidents was used to compute the *a posteriori* error. Monte Carlo simulations were also used to examine the correlation between parameters. Distributions were created with and without the Bayesian term and solving for different numbers of parameters. For typical cases with a normal distribution the correlation coefficient was above 0.9 indicating strong correlation between all pairs of parameters. The result suggests that we may not be able to reliably optimize all parameters from the current data set (see also Wang et al., 2001).

4.2.4. What are the most sensitive parameters in the inversion?. Since parameters were correlated through the inverse procedure, and since there were large errors in the Q_{10} estimate, we need to study systematically what are the most important parameters for matching the data. The inversion procedure was repeated where one to three parameters at a time were kept constant at their original value. ε was always estimated because we already recognized its importance for modelling the NEE diurnal and seasonal amplitude (see Fig. 5). Inspection of χ^2 values given in Fig. 7 show that optimizing Q_{10} does not imply a significant improvement of the quality of the fit. Correcting other maintenance and soil respiration parameters is nearly equally important, and together they have a significant effect on the result. At face value, adjusting ε alone improves χ^2 on average

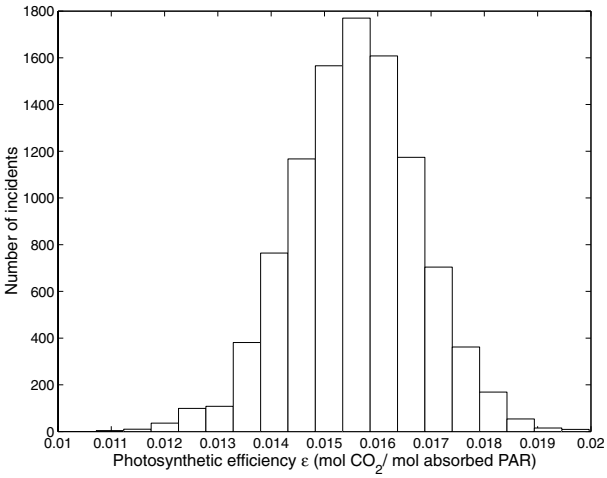

Fig. 6. Distribution of optimized photosynthetic efficiencies at the site GE1 obtained from a set of 10 000 Monte Carlo simulations.

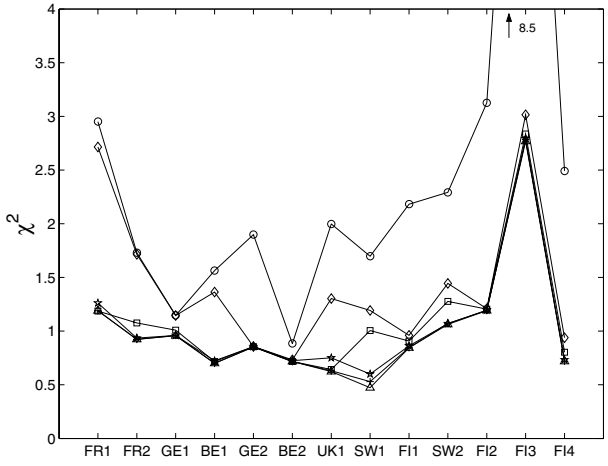

Fig. 7. Difference between *a priori* modelled, optimized and measured fluxes (χ^2, eq. (5)) as a sum over the high growing season. Circles, original parameter set; diamonds, ε optimized; squares, ε and V_0 (soil respiration) optimized; stars, ε and C (maintenance respiration) optimized; plus signs, ε, V_0 and C optimized; triangles, ε, V_0, C and Q_{10} optimized.

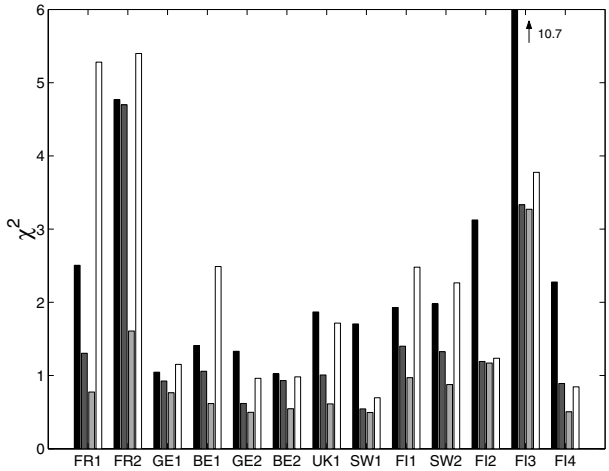

Fig. 8. Difference between observed and measured fluxes (χ^2, eq. (5)) as a sum over the growing season. Colours of the bars from dark to light: original constant parameters; high season constant parameters; individual daily values for parameters; mean of daily parameters.

by 35%, suggesting that the photosynthetic efficiency is indeed the most important parameter in bettering the fit. The optimized value of ε was rather conservative in relation to changes in other parameters. For example, optimization of parameters with and without Q_{10} resulted in a change of less than 0.5% in the value of ε. We noticed, however, an increasing sensitivity of ε going from South to North (Fig. 7): additional adjustment of respiration parameters together with ε resulted in a χ^2 value that was 45% better at southern sites, whereas adjustments of ε alone appeared sufficient for northern sites.

4.2.5. Inversion of daily versus seasonal mean ε. Figure 8 compares the χ^2 returned by the inversion of seasonal $\bar{\varepsilon}$, by the inversion of daily ε, and by replacing in the cost function $\bar{\varepsilon}$ by the average of individual daily values. It can be seen than the χ^2 values for $\bar{\varepsilon}$ are slightly larger than the ones obtained using individual daily ε because of an imperfect fit to the data in spring and autumn. Having to optimize daily ε values in order to better match the data suggests that the TURC model structure itself could be improved, for instance by introducing more degrees of freedom, such as a dependency of ε on more mechanistic physiological parameters. On the other hand, a high growing season constant $\bar{\varepsilon}$ produced considerably better results in comparison to the mean of daily values (Table 2, Fig. 8) when calculating the χ^2 values over the whole growing season. The large χ^2 for FR2 are due to the disagreement between model and data during April and May. The modelled onset of photosynthesis is several weeks ahead of the measurements. Solving for a seasonal $\bar{\varepsilon}$ does not correct for this shortcoming of the model. The forest at FR2 is deciduous while at other sites (except FI3 and FI4) forests are mixed or coniferous. Thus the springtime start at other sites might be less abrupt than at FR2. χ^2 values for FI3 are very high partly due to the low LAI used in the analysis. At FI3 the model and measurements also disagree at the beginning of the growing season (late June) thus resulting in high χ^2 values. The TURC model predicts photosynthetic activity earlier than observed. This can be expected, since the FI3 site consists of peatland while the corresponding 1×1 km NDVI value may be affected by birch populations in the vicinity. FI3 is also the only site where local NDVI is consistently lower than the spatially averaged NDVI suggesting higher photosynthetic activity in the neighbouring grid cells. It is also probable that the melting of snow does not give a wrong NDVI signal during June and July, since there are no reports of snow cover after the last days of May.

The choice of inverting daily photosynthetic efficiencies offers little possibility for extrapolating pointwise NEE data to biomes, as required for atmospheric transport studies. For example, daily photosynthetic efficiencies did not show an obvious relationship between daily irradiation, T_{soil} or T_{air} (correlation coefficients below 0.5). Furthermore, during the start and end of the growing season the differences between model and measurements might be due to processes other than the actual value of ε, which are not explicitly accounted for in TURC. For example, the seeming correlation between photosynthetic efficiency and temperature in Fig. 3 is probably an artefact due to the 10-day averaged NDVI, which could not capture the rapid early spring changes in the climate-driven photosynthesis rates. From the point of view of extrapolating optimized parameters to larger spatial scales, a high growing season constant ε would probably be a more robust choice than the mean of daily values, because the latter is influenced by the start and end of the growing season. Moreover, the mean of daily values does not improve χ^2 compared with a seasonal $\bar{\varepsilon}$ because of the error induced by averaging.

5. Discussion

The measured and *a priori* modelled NEE show significant differences across all sites. The modelled NEE often produces less uptake in the growing season than the measured NEE, especially at northern sites. Such a mismatch can be due to the fact that the spatial scales of the eddy flux measurement and model do not match perfectly. The model is forced by NDVI averaged over 1 × 1 km grid points, whereas the footprint of the eddy covariance measurements extends from few hundred metres to kilometre scale, depending on the wind direction, land cover and topography. The satellite measurements describe only the average results from the grid cell area and from a 10 day-period and therefore, in addition to the photosynthetic efficiency ε, the canopy absorption coefficient f in the model can also be different for individual sites, especially during spring and autumn. Drought effects can also be very local. However, the modelled fluxes are in good agreement with the pointwise observations, and show lower flux values at some northern sites. Furthermore, it is reasonable to optimize ε using eddy covariance measurements since the original values were obtained using measurements of similar scale (Ruimy et al., 1995, 1996b).

Two different inversions of the parameter ε were evaluated. Daily ε produced the best fit to the data, but in large models it may be impractical to determine ε separately for each grid point and for each day. It could be possible to implement a function of new parameters controlling the dependency of ε as a function of climate over the growing season, but the average change is difficult to estimate and the benefits are difficult to prove in this context. The most reasonable solution here was to adjust the high growing season fluxes to the observation, i.e. use a seasonally constant $\bar{\varepsilon}$. On the other hand, daily instead of constant Q_{10} inversion does not produce a significantly better fit of the data. Q_{10} is rather difficult to determine, given its strong correlation with V_0 and the need for relevant soil temperature time-series. It is probable that we are not able to make reliable estimates of Q_{10} in our method. This is not surprising since other models have also shown that only a rather small number of parameters can be estimated from flux data, even when latent and sensible heat data are added to the observation vector in the cost function (Wang et al., 2001).

For a first group of sites, SW1, SW2, FI1, UK1 and GE2, the optimized $\bar{\varepsilon}$ value (average across sites = 0.029) was found to be about twice as high as the original estimate (0.015). Those sites are coniferous and mixed forests aged from 14 to 99 years, with cool annual mean temperatures (1–10 °C). For a second group of sites, GE1, BE1, BE2, FR1 and FR2, the optimized value of $\bar{\varepsilon}$ (0.018) was about the same as the original value. Those sites are coniferous, mixed and deciduous forests at temperate continental and oceanic climates with annual mean temperatures in the range 6–13 °C. Such sites are susceptible to drought stress. Values of 0.02 molCO_2 molPAR^{-1} (Ruimy et al., 1995) and 0.03 mol mol^{-1} (Waring et al., 1995) have been reported for ε. For forests the value might be higher and more variable (e.g. Ruimy et al., 1995). The upper limit of the reasonable variation can probably be set to the leaf level values, which can be of the order of 0.05 mol mol^{-1} (Ehleringer and Pearcy, 1983). Thus the high values that we obtain at the northernmost sites are probably not unrealistic.

A third group of high northern latitude sites consists of FI2, FI4 and FI3. Coniferous species are found only at FI2, where $\bar{\varepsilon}$ is slightly smaller than at other Finnish and Swedish conifer sites. The site FI3 consists of peatland, an ecosystem which was unique in this comparison. However, the ecosystems at FI3 and FI4 are quite similar in terms of soil type, except for the mountain birch population present at FI4. The measured fluxes are slightly higher at FI4, but in general they are relatively similar and small. However, the difference in optimized $\bar{\varepsilon}$ is large (0.01 mol mol^{-1}). This is due to difference in modelled fluxes which in turn are affected by LAI values of 2.5 at FI4 and an extremely low value of 0.7 at FI3. These LAI values give 0.74 for $f_{\max}$ at FI4 and only 0.33 at FI3 suggesting need for revision of the LAI index at the FI3 site or revision of the f function at very low values of LAI (see Fig. 4e in Brown et al., 2000). The estimates for FI2 and FI4 should be considered with great care, since the measurement period for FI2 lasted only 2 weeks and the measurements for FI4 were made during 1996. The NDVI index could therefore be different from reality. However, it is probable that the average level of the fluxes is the same during both years. For FI2 it is probable that the level of maximum fluxes was reached during the measurement period, since there was no drought before or during the period, and near optimal irradiance and temperature conditions were recorded. The local NDVI values also indicate that the period of maximum fluxes was captured.

The highest $\bar{\varepsilon}$ was obtained for SW1, an old coniferous forest in Southern Sweden which has experienced significant disturbance (soil drainage). Other sites have also been managed (e.g. UK1 by ploughing, fertilization). These actions have earlier been shown to be important in regulating the ecosystem flux balance by, for example, changing the relative contributions of respiration and GPP in the carbon budget (Janssens et al., 2001). GPP, on the other hand, has been suggested to be relatively constant over latitudinal gradient (Valentini et al., 2000) except for the intensively managed forest in UK1 showing high uptake rates. Our preliminary analysis, using the optimized $\bar{\varepsilon}$ together with NDVI from TURC and the gridded climate fields from April to October calculated by the mesoscale climate model REMO (Chevillard et al., 2002), also suggests only a weak dependence of GPP over latitude, except for the three northernmost sites FI2, FI3 and FI4 which show clearly lower GPP values. These sites were not included in the analysis of Valentini et al. (2000).

According to the current dataset the photosynthetic efficiency is very difficult to express as a function of tree age or classified according to species. The performance of the TURC model would, however, be better if ε is reparametrized, especially at northern

sites. The easiest possibility would be to use the current function with a small upward adjustment for northern conifers (see ε as a function of latitude in Fig. 4b). This proposed modification would result in a change in the large scale patterns of fluxes in the TURC model that can be verified independently by detailed comparison with atmospheric measurements.

6. Acknowledgments

The pleasant co-operation with the CARBOEUROFLUX research community (especially Mika Aurela, Eva Falge, Tuomas Laurila, Tanja Suni and Timo Vesala) who provided the measurement data is acknowledged. We are very grateful to Philippes Bousquet and Peylin for their input on the inverse procedure. The NDVI data were efficiently provided by the VITO data centre (Dirk Van Speybroeck, M. Veroustraete) and biomass maps by Sebastien Lafont. The financial support from the Academy of Finland is gratefully acknowledged.

References

Aalto, T., Hatakka, J., Paatero, J., Tuovinen, J.-P., Aurela, M., Laurila, T., Holmen, K., Trivett, N. and Viisanen, Y. 2002. Tropospheric carbon dioxide concentrations at a northern boreal site in Finland: Basic variations and source areas. *Tellus* **54B**, 110–126.

Aubinet, M., Grelle, A., Ibrom., A., Rannik, Ü., Moncrieff, J., Foken, T., Kowalski, A. S., Martin, P. H., Berbigier, P., Bernhofer, C., Clement, R., Elbers, I., Granier, A., Grünwald, T., Morgenstern, K., Pilegaard, K., Rebmann, C., Snijders, W., Valentini, R. and Vesala, T. 2000. Estimates of the annual net carbon and water exchange of forests: the EUROFLUX methodology. *Adv. Ecol. Res.* **30**, 113–175.

Aurela, M., Laurila, T. and Tuovinen, J.-P. 2001a. Seasonal CO_2 balances of a subarctic mire. *J. Geophys. Res.-Atmos.* **106**, 1623–1637.

Aurela, M., Tuovinen, J.-P. and Laurila, T. 2001b. Net CO_2 exchange of a subarctic mountain birch ecosystem. *Theor. Appl. Clim.* **70**(1–4), 135–148.

Baldocchi, D.D., Falge, E., Gu, L., Olson, R., Hollinger, D., Running, S., Anthoni, P., Bernhofer, Ch., Davis, K., Fuentes, J., Goldstein, A., Katul, G., Law, B., Lee, X., Malhi, Y., Meyers, T., Munger, J. W., Oechel, W., Pilegaard, K., Schmid, H. P., Valentini, R., Verma, S., Vesala, T., Wilson, K. and Wofsy, S. 2001. FLUXNET: a new tool to study the temporal and spatial variability of ecosystem-scale carbon dioxide, water vapor and energy flux densities. *Bull. Am. Meteorol. Soc.* **82**, 2415–2435.

Barlow, R. 1993. *Statistics: a Guide to the Use of Statistical Methods in the Physical Sciences.* John Wiley, New York.

Berbigier, P., Bonnefond, J.-M. and Mellman, P. 2001. CO_2 and water vapour fluxes for 2 years above Euroflux forest site. *Agric. Forest Meteorol.* **108**, 183–197.

Boone, R. D., Nadelhoffer, K. J., Canary, J. D and Kaye, J. P. 1998. Roots exert a strong influence on the temperature sensitivity of soil respiration. *Nature* **396**, 570–572.

Brown, L., Chen, J. M., Leblanc, S. G. and Cihlar, J. 2000. A shortwave infrared modification to the simple ration for LAI retrieval in boreal forests: an image and model results. *Remote Sens. Environ.* **71**, 16–25.

Chevillard, A., Karstens, U., Ciais, P., Lafont, S. and Heimann, M. 2002. Simulation of atmospheric CO_2 transport in Europe and Siberia using the regional scale model REMO. *Tellus* **54B**, 872–895.

Ciais, P., Brandt, J., Koerner, S., Heimann, M., Aalto, T., Bousquet, P., Chevillard, A., Christensen, J. H., Frohn, L. M., Geels, C., Gloor, M., Gusti, M., Houwelling, S., Karstens, U., Peylin, P., Roedenbeck, C., Vermeulen, A. and Denning, A. S. 2002. Intercomparison of simulated transport of CO_2 and ^{222}Rn over Europe with mesoscale models: a concerted action within the AEROCARB project. *Eos Transact. AGU,* **83**(19), Spring Meeting Supplement, Abstract B51A-06.

Cramer, W., Kicklighter, D. W., Bondeau, A., Moore, B., Churkina, G., Nemry, B., Ruimy, A., Schloss, A. L. and The Participants of the Potsdam NPP Model Intercomparison. 1999. Comparing global models of terrestrial net primary productivity (NPP): overview and key results. *Global Change Biol.* **5** (Suppl. 1), 1–15.

Ehleringer, J. and Pearcy, R. W. 1983. Variations in quantum yield for CO_2 uptake among C3 and C4 plants. *Plant Physiol.* **73**, 555–559.

Eklundh, L., Harrie, L. and Kuusk, A. 2001. Investigating relationships between Landsat ETM+ sensor data and leaf area index in a boreal conifer forest. *Remote Sensing Environ.* **78**, 239–251.

Granier, A., Ceschia, E. and Damesin, C. 2000. The carbon balance of a young beech forest. *Funct. Ecol.* **14**, 312–325.

Gurney, K., Law, R., Denning, S., Rayner, P., Baker, D., Bousquet, P., Bruhwiler, L., Chen, Y.-H., Ciais, P., Fan, S., Fung, I., Gloor, M., Heimann, M., Higuchi, K., John, J., Maki, T., Maksyutov, S., Masarie, K., Peylin, P., Prather, M., Pak, B., Randerson, J., Sarmiento, J., Taguchi, S., Takahashi, T. and Yuen, C.-W. 2002. Towards robust regional estimates of CO_2 sources and sinks using atmospheric transport models. *Nature* **415**, 626–630.

Janssens, A., Lankreijer, H., Matteucci, G., Kowalski, A. S., Buchmann, N., Epron, D., Pilegaard, K., Kutsch, W., Longdoz, B., Grunwald, T., Montagnani, L., Dore, S., Rebmann, C., Oltchev, S., Clement, R., Gudmundsson, J., Minerbi, S., Berbigier, P., Ibrom, A., Moncrieff, J., Aubinet, M., Bernhofer, C., Jensen, N. O., Vesala, T., Granier, A., Schulze, E. D., Lindroth, A., Dolman, A. J., Jarvis, P., Ceulemans, R. and Valentini, R. 2001. Productivity overshadows temperature in determining soil and ecosystem respiration across European forests. *Global Change Biol.* **7**, 269–278.

Jarvis, P. G. and Leverenz, J. W. 1983. Productivity of temperate, deciduous and evergreen forests. In: *Physiological Plant Ecology IV. Encyclopedia of Plant Physiology* (eds Lange, O. L. et al.), Springer, Berlin, 233–280.

Kindermann, J., Badeck, F.-W., Wurth, G. and Kohlmaier, G. H. 1996. Interannual variation of carbon exchange fluxes in terrestrial ecosystems. *Global Biogeochem. Cycles* **10**, 737–746.

Kowalski, A. S., Overloop, S. and Ceulemans, R. 1999. Eddy fluxes above a Belgian, Campine forest and their relationship with predicting variables. In: *Forest Ecosystem Modelling, Upscaling and Remote Sensing* (eds Ceulemans, R. et al.), SPB Academic Publishing, The Hague, 3–18.

Lafont, S., Kergoat, L., Dedieu, G., Chevillard, A., Karstens, U. and Kolle, O. 2002. Spatial and temporal variability of land CO_2 fluxes estimated with remote sensing and analysis data over western Eurasia. *Tellus* **54B**, 820–834.

Lindroth, A., Grelle, A. and Moren, A.-S. 1998. Long-term measurements of boreal forest carbon balance reveal large temperature sensitivity. *Global Change Biol.* **4**, 443–450.

Lloyd, J. and Taylor, J. A. 1994. On the temperature dependence of soil respiration. *Funct. Ecol.* **8**, 315–323.

Maisongrande, P., Ruimy, A., Dedieu, G. and Saugier, B. 1995. Monitoring seasonal and interannual variations of gross primary productivity, net primary productivity and net ecosystem productivity using a diagnostic model and remotely sensed data. *Tellus* **47B**, 178–190.

Markkanen, T., Rannik, U., Keronen, P., Suni, T. and Vesala, T. 2001. Eddy covariance fluxes over a boreal Scots pine forest. *Boreal Environ. Res.* **6**, 65–78.

McGuire, A. D. C., Sitch, S., Clein, J. S., Dargaville, R., Esser, G., Foley, J., Heimann, M., Joos, F., Kaplan, J., Kicklighter, D. W., Meier, R. A., Melillo, J. M., Moore, B., Prentice, I. C., Ramankutty, N., Reichenau, T., Schloss, A., Tian, H., Williams, L. J. and Wittenberg, U. 2001. Carbon balance of the terrestrial biosphere in the twentieth century: Analysis of CO2 climate and land use effects with four process-based ecosystem models. *Global Biogeochem. Cycles* **15**, 183–206.

Pacala, S. W., Hurtt, G. C., Baker, D., Peylin, P., Houghton, R. A., Birdsey, R. A., Heath, L., Sundquist, E. T., Stallard, R. F., Ciais, P., Moorcroft, P., Caspersen, J. P., Shevliakova, E., Moore, B., Kohlmaier, G., Holland, E., Gloor, M., Harmon, M. E., Fan, S. M., Sarmiento, J. L., Goodale, C. L., Schimel, D. and Field, C. B. 2001. Consistent land- and atmosphere-based U.S. carbon sink estimates. *Science* **292**, 2316–2320.

Prince, S. D. 1991. A model of regional primary productivity for use with coarse resolution satellite data. *Int. J. Remote Sens.* **12**, 1313–1330.

Raich, J. W. and Schlesinger, W. H. 1992. The global carbon dioxide flux in soil respiration and its relationship to vegetation and climate. *Tellus* **44B**, 81–99.

Roderick, M. L., Farquhar, G. D., Berry, S. L. and Noble, I. R. 2001. On the direct effect of clouds and atmospheric particles on the productivity and structure of vegetation. *Oecologia* **129**, 21–30.

Ruimy, A., Saugier, B. and Dedieu, G. 1994. Methodology for the estimation of net primary production from remotely sensed data. *J. Geophys. Res.-Atmos.* **99**, 5263–5283.

Ruimy, A., Jarvis, P. G., Baldocchi, D. D. and Saugier, B. 1995. CO_2 fluxes over plant canopies and solar radiation: a review. *Adv. Ecol. Res.* **26**, 1–68.

Ruimy, A., Dedieu, G. and Saugier, B. 1996a. TURC: A diagnostic model of continental gross primary productivity and net primary productivity. *Global Biogeochem. Cycles* **10**, 269–286.

Ruimy, A., Kergoat, L., Field, C. B. and Saugier, B. 1996b. The use of CO_2 flux measurements in models of the global terrestrial carbon budget. *Global Change Biol.* **2**, 287–296.

Tarantola, A. 1994. *Inverse Problem Theory: Methods for Data Fitting and Model Parameter Estimation*, Elsevier, Amsterdam, The Netherlands, 600 pp.

Valentini, R., Matteucci, G., Dolman, A. J., Schulze, E.-D., Rebmann, C., Moors E. J., Granier, A., Gross, P., Jensen, N. O., Pilegaard, K., Lindroth, A., Grelle A., Bernhofer, C., Grunwald, T., Aubinet, M., Ceulemans, R., Kowalski, A. S., Vesala, T., Rannik, U., Berbigier, P., Loustau, D., Gudmundsson, J., Thorgeirsson H., Ibrom, A., Morgenstern, K., Clement, R., Moncrieff, J., Montagnani, L., Minerbi, S. and Jarvis, P. G. 2000. Respiration as the main determinant of carbon balance in European forests. *Nature* **404**, 861–864.

Valentini, R. Ed. 2003. *Fluxes of Carbon, Water and Energy of European Forests, Ecological Studies 163*, Springer, Berlin. 260 pp.

Wang, Y. P., Leuning, R., Cleugh, H. A. and Coppin, P. A. 2001. Parameter estimation in surface exchange models using nonlinear inversion: how many parameters can we estimate and which measurements are most useful? *Global Change Biol.* **7**, 495–510.

Waring, R. H., Law, B. E., Goulden, M. L., Bassow, S. L., McGreight, R. W., Wofsy S. C. and Bazzaz, F. A. 1995. Scaling gross ecosystem production at Harvard Forest with remote sensing: a comparison of estimates from a constrained quantum-use efficiency mode and eddy correlation. *Plant Cell Environ.* **18**, 1201–1213.